DOI: https://doi.org/10.2138/am-2018-6462

MSA Award Lecture: An accessory mineral and experimental perspective on the evolution of the early crust.

Dustin Trail

`

Revision #1

March 7th, 2018

Department of Earth & Environmental Sciences
University of Rochester, Rochester, NY 14627, USA

Department of Earth, Planetary and Space Sciences,
University of California, Los Angeles, CA, USA

dtrail@ur.rochester.edu; ph 585 276 7182

This is a preprint, the final version is subject to change, of the American Mineralogist (MSA)
Cite as Authors (Year) Title. American Mineralogist, in press.
DOI: https://doi.org/10.2138/am-2018-6462

Abstract. As the only known mineral with confirmed ages >4 Ga, zircon is unmatched in the field of early Earth research. In the past two decades, researchers have continued to establish connections between zircon chemistry and the physical/chemical processes that shaped the early crust. This connection has benefited greatly from the application of high temperature/pressure laboratory experiments. This study presents: (i) new zircon U-Pb geochronology and strategies for characterizing and identifying ancient terrestrial material from the Inukjuak Domain in northern Québec, and the Jack Hills, Western Australia; and (ii) a blend of new laboratory experiments and measurements of isotope ratios and trace impurities of natural zircon. Research directions in need of future exploration, with emphasis on early Earth studies, are also explored. Topics include Hadean hydrous magmatism and the structural accommodation of "water" into the zircon lattice, Hadean subaerial crust and the identification of peraluminous or metaluminous source melts, methods to characterize the oxidation state of magmas and fluids, and the complementarity of the Si- and O- isotopic systems as proxies for crustal weathering. Finally, the implications of this work are discussed in the context of a possible transition from prebiotic to biotic chemistry on the early Earth.

48

49 # Introduction

50 Zircon ($ZrSiO_4$) is an excellent carrier of geochemical information through time; in many
51 ways, it is unsurpassed in its physical and chemical durability, and it is readily dated because it
52 incorporates U and Th which decay to isotopes of Pb. It is because of this robustness that
53 zircons are often found in sediments. The mere presence of this mineral is not diagnostic or
54 unique to any specific rock type, tectonic setting, or environment; zircons occur in the
55 continental and oceanic crust, in kimberlites, and in some meteorites and lunar rocks (Ireland and
56 Wlotzka, 1992; Valley et al., 1998; Watson et al., 2006; de Hoog et al. 2014; Barboni et al.,
57 2017). It is because zircons do crystallize in diverse settings that researchers have turned to the
58 investigation of trace element chemistry and key isotopic ratios as proxies for their formation
59 environment.

60 The importance is amplified because detrital zircons yield ages as old as ~4.4 Ga, which
61 exceeds the age of the oldest known, widely agreed upon rock by about 400 million years (Maas
62 et al., 1992; Wilde et al., 2001; Mojzsis et al., 2001; Holden et al., 2009; Thern et al., 2012;
63 Mojzsis et al., 2014). Over the past two decades, numerous geochemical investigations of
64 Hadean zircon (>4.0 Ga) have been conducted (e.g., Wilde et al., 2001; Mojzsis et al., 2001;
65 Cavosie et al., 2005, 2006; Trail et al., 2007; Harrison et al., 2008; Hopkins et al., 2008; Bell et
66 al., 2011, 2017; Harrison et al., 2017). These studies, which are mainly based on measurements
67 of: (i) oxygen and hafnium isotope ratios; (ii) rare earth element (REE) contents; and (iii) the
68 composition of other minerals (inclusions) found within the zircons, have led researchers to
69 conclude that the early Earth contained an evolved rock cycle including water-rock interaction,
70 formation of granitic crust and probable sediment cycling. The above studies typically utilized

experimental zircon diffusion data (see Cherniak, 2010) to argue for primary retention of trace element contents and isotope ratios of ancient grains.

In a generally different strategy, researchers sought to develop zircon-based calibrations in the controlled setting of an experimental geochemistry laboratory. Such experiments have played a fundamental role in the quest to link chemical signatures preserved in ancient zircons with Hadean processes. For instance, the Ti content of zircon was calibrated as an indicator of a zircon's crystallization temperature and zircon Ce anomalies were investigated as a proxy for redox conditions of early Earth magmas (Watson and Harrison, 2005; Watson et al., 2006; Ferry and Watson, 2007; Trail et al., 2011a; Trail et al., 2012). This work led to new discoveries about the early Earth, including evidence for water-saturated or near water-saturated Hadean magmas, and suggestions that Hadean volcanic emanations that were broadly neutral (e.g., CO_2) rather than uniformly reduced (e.g., CO).

This paper presents new data, some speculations, and highlights a handful of research directions that are presently of interest to the author. With little deviation, this contribution explores the chemistry of the terrestrial zircon age end-members. A progress report is presented for zircon U-Pb geochronology studies of the Inukjuak Domain and the Jack Hills aimed at identifying the oldest terrestrial zircons and new fragments of ancient crust. The chemistry of the youngest, newly-formed crystals from laboratory experiments are discussed in the context of the chemistry of the oldest detrital Eoarchean and Hadean zircons. Many of the topics explored are relevant to origin(s) of life questions and planetary habitability. Such discussions will remain important as evidence for an early terrestrial biosphere continue to mount.

Eoarchean and Hadean material.

94 **Inukjuak domain**

95 Rocks hosting Eoarchean zircons outcrop approximately 30 km south of Inukjuak (town),
96 near to Porpoise Cove on the eastern shore of Hudson Bay, located at the western edge of the
97 Northeast Superior Province in northern Quebec, Canada (David et al., 2009; Cates and Mojzsis,
98 2009; Cates et al., 2013; Darling et al., 2013). Thus far, well studied rocks in the region include
99 the Nuvvuagittuq Supracrustal Belt (NSB) with amphibolite supracrustal rocks, rare felsic
100 schists, possible conglomeratic units, oxide-rich and quartz-rich iron formations, all of which is
101 surrounded by Archean granitoid gneisses. The NSB surrounds tonalites which yield ages from
102 3.4 to 3.66 Ga (David et al., 2009; O'Neil et al., 2013). The felsic schist and conglomeritic units
103 within in the NSB contain detrital zircons with U-Pb or Pb-Pb depth profile ages of ~3.7-3.8 Ga
104 (David et al., 2009; Cates and Mojzsis, 2009; Cates et al., 2013), constraining the emplacement
105 age of the NSB to the Eoarchean (Cates et al., 2013). Others have suggested that the rocks
106 hosting these zircons are not sedimentary, but igneous intrusions, and that the NSB is ≥4.2 Ga
107 (e.g., Darling et al., 2013).

108 O'Neil et al. (2008) discovered NSB cummingtonite-rich amphibolites record deficits in
109 the daughter product (^{142}Nd) of the extinct radionuclide ^{146}Sm. These deficits require isolation of
110 an enriched low Sm/Nd crustal source of these rocks from the ^{142}Nd isotopic evolution of the
111 bulk silicate earth in the first few hundred million years of Earth history. More recently, Caro et
112 al. (2017) conducted ^{146}Sm-^{142}Nd and ^{147}Sm-^{143}Nd measurements on samples from the Ukaliq
113 Supracrustal Belt (USB) a few km northeast of the NSB. These authors report the discovery of
114 amphibolites with ^{142}Nd/^{144}Nd deficits. Caro et al. (2017) favor inheritance from an enriched
115 mantle source as the explanation for the USB and NSB ^{142}Nd/^{144}Nd deficits (cf. O' Neil et al.,
116 2008, 2013). Even though there is not yet consensus about the meaning of ^{142}Nd/^{144}Nd

anomalies in this domain, their discovery is extremely important to early earth geology, and has led to a discussion about the possible preservation and volume of Hadean crust this remote area.

The remoteness and challenges involved in sampling of this region perhaps warrant other exploration strategies. One possibility investigated here involves the collection of loose, unconsolidated sediments in strategic areas away from the present-day shore of the Hudson Bay. This tactic is based on the premise that such sediments are broadly regionally sourced, or at least are not dominated by loess or glacial till. In other words, unconsolidated sediments "sample" larger areas than possible with single hand samples, though in broadly restricted areas that may become the target of more intensive follow-up studies. This approach was tested in this domain for a few reasons. First, there is evidence for Eoarchean materials, and chemical signatures that have origins in the Hadean. Second, the rocks are reasonably well studied, in that the ages of the exposed surface area are broadly characterized. And finally, the younger Voizel suite contains inherited $^{142}Nd/^{144}Nd$ deficits implying Hadean chemical remnants (O'Neil et al., 2008; Roth et al., 2013; Caro et al., 2017).

Unconsolidated sediment samples were collected during the July of 2016 field season. I226 and I247 were sampled in the NSB from small streams about 1 meter across and less than 1 meter deep. I300 was collected from the shores of a small lake with a surface area of ~0.5 km, just to the east of the USB (**Figure 1**). Sediment samples were sieved and processed for zircon following standard heavy mineral separation procedures (e.g., Cates and Mojzsis, 2009; Trail et al., 2017). In this reconnaissance investigation, about 100 or more zircons from each of three samples were mounted on double-sided tape. Grains were cast in epoxy, polished to expose the cores, and U-Pb dated by LA-ICP-MS following the same procedure discussed in Trail et al. (2017). Briefly U-Pb data were collected with a Photon Machines 193 nm laser (25 μm spot)

coupled to an Agilent 7900 quadrupole mass spectrometer, with ages standardized against AS-3 zircon (Paces and Miller, 1993).

As expected, NSB stream samples yield U-Pb zircon ages dominated by the 2.7 Ga Boizard suite (**Figure 2**). Some ages are in broad agreement with Voizel suite and central tonalite ages (3.4 to 3.66 Ga). Note, however, that none of the ~3.7-3.8 Ga NSB zircon ages documented by others (e.g., David et al. 2009; Cates et al. 2013) have yet been discovered in these stream samples. Perhaps the most intriguing datum is from sediment sample I300, collected outside the NSB, which yielded a zircon age of 3740 Ma. The I300 sample was collected south and east of the area mapped by Caro et al. (2017), in which $^{142}Nd/^{144}Nd$ anomalies were identified. The importance of this find suggests that, like the NSB, this newly-documented supracrustal sequence may contain felsic rocks with Eoarchean zircon. On average, this small lake is likely to imply limited transport distance compared to the small stream samples collected (I226 and I247). There are two main outcomes from this reconnaissance sampling style in the Inukjuak domain. First, even low flow steam samples may prove too challenging to trace the origins rocks samples (I226 and I247), but this needs to be taken in context as only limited geochronology has been conducted. Second, the I300 sample predicts a hereto unreported felsic component in the USB that hosts >3.7 Ga zircons.

Jack Hills

If zircon U-Pb geochronology is the criterion, then the Jack Hills classic locality metasedimentary outcrop, located in Western Australia, is the most well studied site in the world. Holden et al. (2009) presented a strategy and design for rapid Pb-Pb survey and U–Pb zircon age determination, using an automated ion microprobe. Thus far, approximately 200,000 zircons

been screened using this technique, with approximately 6000 grains yielding ages older than 4.0 Ga (Harrison et al., 2017). Since the above Hadean zircon search commenced, advances in LA-ICP-MS (laser ablation inductively coupled plasma mass spectrometry) technology make it a viable geochronology alternative under certain circumstances.

Trail et al. (2017) presented U-Pb geochronology and other trace element data, for Jack Hills zircons by LA-ICP-MS. In this study of 275 zircons, ~12% of the grains are >4.0 Ga (**Figure 3a**). The volume of removed material is ~5000 um^3, leaving up to or greater than 90% of the sectioned grain for follow-up geochemical studies. Grains may be subsequently polished, leaving only the remaining outline of the ablation pits, if desired (**Figure 3b**). Consistent with previous results, a large fraction of the JH detrital zircon population is Paleoarchean, with an age peak centered at about 3.35 Ga. These Archean grains may be of value for certain studies (Bell et al., 2011), though the demand for such samples is diminished due to the presence of rocks of this age.

For those studies whose goal is to explore Hadean Earth, one possible Hadean zircon "concentration" strategy presently under exploration involves placing zircons mounted on double-sided tape directly into the same chamber of the LA instrument. Zircons remain unpolished and are not cast in epoxy. Approximately 1500 zircons from the same JH mineral separate as above were U-Pb dated at the University of Rochester (**Figure 3c,d**). Results reveal that 76/1514, or about 5% of the grains are older than 4.0 Ga. When compared to the previous data set, there is a shift in the peak of the old age population from 4.05 Ga (Figure 3a), to ~3.95 Ga (Figure 3c). Moreover, a larger percentage of the apparent age population plot in the 3.8 to 4.0 Ga interval. If these grains are included in the old age population, then the total increases

from 76/1514 to 173/1514 (or 11% of the population), which is comparable to the polished zircon U-Pb geochronology presented in Figure 3a.

Both zircon aliquots are from the heavy mineral separate and were picked from fresh separate. It is therefore reasonable to speculate that many of the unpolished grains with apparent ages between 3.8 to 4.0 Ga represent younger age domains or Pb loss mixed with older cores. This observation is consistent with Pb-Pb depth profiling and U-Pb spot mode geochronology conducted on Jack Hills zircons (e.g., Cavosie et al., 2004; Trail et al., 2007; Abbott et al., 2012). Since these zircons remain attached only to tape, the plan is to target grains with apparent ages older than 3.8 Ga. Samples will be mounted in epoxy, and prepared for follow-up U-Pb or stable isotope investigations. This strategy has clear advantages. First, a high percentage of ancient grains may be mounted in very close proximity to standards – a desired feature for ion microprobe work (e.g., Kita et al., 2009) – with relatively little effort. Second, in cases where a certain mass of Hadean material is required for a trace element or isotope measurement (e.g., Amelin, 2004), ~90% of the original grain is retained and may be simply removed from the double-sided tape.

Experiments and applications

Hydrous magmatism.

Several lines of evidence imply the presence of hydrous magmatism on the early Earth, including zircon crystallization temperatures, oxygen isotopes that are fractionated away from the canonical mantle values, and inclusions assemblages, such as muscovite (Wilde et al., 2001; Mojzsis et al., 2001; Watson and Harrison, 2005; Hopkins et al., 2008; Harrison, 2009). Yet, a

calibration that enables direct quantification of the water activity of magmas through the analysis of zircon chemistry is not available. Trail at al. (2011b) conducted experiments in the H_2O-SiO_2-ZrO_2 system, at 1650 and 1550 ^oC, and found that "water" – or OH – can be structurally accommodated by the zircon lattice. The OH measurements were performed by Fourier Transform Infrared (FTIR) spectroscopy and H_2O concentrations were quantified using the following relationship:

$$c(wt\%H_2O) = \frac{A_i(cm^{-1}) * 1.8015}{t(cm) \cdot D(g/cm^3) \cdot \varepsilon_i(cm^{-2}\, per\, mol\, H_2O/L)}$$

where c is concentration, A_i is the total integrated area in the OH stretching region, t is the sample thickness, D is the density of zircon (4.65 g/cm^3), and ε_i is the absorption coefficient. de Hoog et al. (2014) suggested that the absorption coefficient used in this study and reported by Bell et al. (2004) may be different than the true value by a factor of 2, and should be revisited. Thus, new data presented below are reported as total integrated area (A_i; see Trail et al. 2011b for additional details), with rare references to concentration.

Trail et al. (2011b) did not rigorously establish a relationship between the solubility of water in zircon and temperature. Those results however, do suggest this relationship does exist, with measurable differences in the H_2O concentration detected for 1650 and 1550 ^oC experiments. New data for zircon synthesized in the H_2O-SiO_2-ZrO_2 system are plotted as log(A_i, per mm of zircon thickness) vs. 10^3/T(K) and reveal an inverse relationship (**Figure 4**). Accepting for the moment that these experiments have water activities close to unity, then extrapolation of these data down to 700 ^oC predicts a solubility of 0.5 to 10 ppm H_2O in zircon. This range of concentration includes propagation of fitting errors (see Figure 4), and assumes a factor of 2 uncertainty in ε_i. Silicate melts with water activities lower than one will lower the

apparent concentration further. While measuring such low concentrations will be challenging, this is unlikely the largest issue. Trail et al. (2011b) and de Hoog et al. (2014) demonstrated that H^+ charge couples with trivalent cations, such as the rare earth elements, Y, and Al. Such charge coupling can lead to H_2O concentrations 2-3 orders of magnitude higher than "pure" zircon. This would, in principle, need to be subtracted out to yield results that bear specifically on water activity of the crystallization environment.

This problem of quantifying water activity from ancient zircon with this strategy is further hindered because radiation damaged grains commonly contain secondary H_2O not bound to the lattice (e.g., Woodhead et al. 1991). To demonstrate some of these complexities, new polarized FTIR spectra for synthetic and Jack Hills (JH) zircons are presented (**Figure 5**). Zircons were double polished, and then aligned along principal crystallographic axes before collecting polarized spectra. The synthetic zircon contains absorption bands that change in intensity as a function of crystallographic orientation, strong evidence that H_2O is indeed associated with the zircon lattice. Several other examples representing lattice bound H_2O in zircon are provided in other studies (e.g., Trail et al. 2011b; de Hoog et al. 2014). These results contrast with the two polarized spectra collected //a and //c for the JH zircon. Subtle differences in the absorption features may indicate trace amounts of water present within lattice, but absorption intensity is dominated by isotropic (secondary) water.

However, some of these complexities may be irrelevant for certain types of zircon. Consider, for example, zircons found in kimberlites which are trace element poor and contain low actinide concentrations. In this case, the relationship between H_2O solubility and water activity is likely to be more straightforward. Crystals from African kimberlites Kimberley Pool, South Africa, and Orapa, Botswana (Haggerty et al. 1983) were characterized by FTIR from core

to rim (**Figure 6**). The Orapa zircon, with a radius of about half that of the other sample, exhibit no significant change in the H_2O concentration from rim to core. On the other hand, the Kimberley Pool crystal exhibits a broadly systematic decrease in H_2O contents from rim to core. It is at least possible that the results for the Kimberley Pool zircon represent a diffusion profile, in which case a systematic study to characterize H diffusion in zircon would be extremely valuable as a geospeedometer under certain circumstances. Qualitatively, the results imply that this zircon retains a record of different chemical potentials for H_2O, perhaps related to differences of the H_2O activity of the zircon source region and the mantle source region of the kimberlite. Quantitative constraints will require additional work. For instance, since H_2O solubility in zircon is a function of temperature, the crystallization temperatures will need to be constrained. Estimates of Ti-in-zircon temperatures for mantle zircons (Page et al. 2007) may be complicated by cation site exchange of Ti from the Si site (Tailby et al. 2011; Ferry and Watson, 2007) to the Zr site as a function of pressure (Ferriss et al. 2008). Thus, the solubility of H_2O in zircon is at least a function of temperature, water activity, and trace element composition. Based on very limited experiments – 1.5 and 2.5 GPa only – no pressure-dependent solubility is observed (Trail et al., 2011b) though this needs to be addressed in more detail. Such constraints may help constrain the water activity of these zircon source regions.

Oxidation state of magmas and fluids

The oxygen fugacity (f_{O_2}) of a magma or fluid influences mineral saturation and stability, the viscosity of magmas, and controls the speciation of volatiles in the C-O-H-S system (Carmichael and Ghiorso, 1990; Frost, 1991; Connolly and Cesare, 1993). Oxygen fugacity also defines the molecular speciation of gases exsolved during a volcanic eruption. Trail et al.

(2011a, 2012) showed that redox-sensitive Ce uptake in zircon was systematically sensitive to f_{O_2} and temperature, and as such, a Ce zircon anomaly – defined as the abundance of Ce relative to bracketing REEs La and Pr – was proposed to form the basis of an f_{O_2} sensor for zircon-bearing igneous rocks. Ce^{4+} is more compatible in the zircon lattice (vs. Ce^{3+}), which is due to: (i) the smaller ionic radius of Ce^{4+} (Ce^{4+} = 0.97 Å vs. Ce^{3+} = 1.143; Shannon 1976), which means that Ce^{4+} more readily substitutes for Zr^{4+} (0.84 Å); and (ii) the absence of a charge-balancing cation required for Ce^{4+} in zircon. This work enabled a broad estimate of the oxidation state of Hadean magmas. Magmatic outgassing throughout Earth history is at least partially responsible for the chemical state of the surface environment (Kasting, 1993; Canil, 1997; Delano, 2001; Burgisser, and Scaillet, 2007; Trail et al., 2011a). The variable compatibility of Ce vs. f_{O_2} (Trail et al., 2011a, 2012; Burnham and Berry, 2012), led to the discovery that Hadean (≥4.0 Ga) zircon source melts were not as reduced as lunar samples, but ranged up to values closer to the redox state of modern day magmas (Trail et al. 2011a).

Alternative approaches include direct detection of Ce^{4+}/Ce^{3+} by X-ray Absorption Near Edge Structure (XANES) in zircon (Trail et al. 2015). This approach holds some advantages over other techniques because it relies directly on the chemistry of zircon (cf. Smythe and Brenan, 2016), and Ce valence is expected to be independent of concentration, meaning that there is no need to "normalize" Ce contents against other La, Pr, or other REEs. Bishop Tuff zircons contain systematic core-to-rim zoning in Ce valence, where core regions range from ~40-60 % Ce^{4+}, and zircon rims range from ~70-100 % Ce^{4+}, with errors of ~5% of the absolute scale (Trail et al., 2015). However, Ce valence needs to be mapped onto f_{O_2} before robust quantitative constraints are possible.

298 Experiments reported here suggest it is possible to calibrate the relationship between
299 oxygen fugacity and a direct Ce valence measurement in zircon. Zircon crystals were
300 synthesized in the ZrO_2-SiO_2-H_2O-CeO_2 system at 1125°C and 10 kbar in a piston cylinder,
301 which implies the following substitution mechanism $Zr^{4+} \rightarrow Ce^{3+} + H^+$, after Trail et al. (2011b).
302 The experiments were f_{O_2}-buffered after a design presented in Trail et al. (2012) and Trail
303 (2018). Cerium L_3 edge XANES spectra were collected at Beamline 13 ID-E (GSECARS), at
304 the 7 GeV Advanced Photon Source (APS), Argonne National Laboratory after the technique
305 described in Trail et al. (2015). Briefly, the incident X-ray energy was selected using a Si (111)
306 double crystal monochromator; each spectrum required ~15 minutes to collect. Randomly
307 selected grains from each experiment were analyzed and valence calculated from the Ce^{3+} and
308 Ce^{4+} end-member compounds $Ce^{3+}PO_4$ and $Ce^{4+}SiO_4$, respectively (**Figure 6**). At an f_{O_2} of
309 approximately 6.8 log units above the fayalite-magnetite-quartz equilibrium (FMQ+6.8), >90%
310 of the Ce measured in the zircon crystal is in the tetravalent state. At an f_{O_2} of FMQ+0.7,
311 approximately 60% of Ce is present as Ce^{4+}, with the percentage dropping to ~10% at an f_{O_2}
312 close to the iron-wüstite equilibrium.

313 While promising, there are several areas that will be need to be explored to extract useful
314 oxygen fugacity information from Ce valence measurements in natural zircons. For instance,
315 measured Ce valence within a zircon at a given oxygen fugacity may depend on the substitution
316 mechanism for Ce^{3+}, where the above experiments imply $Zr^{4+} \rightarrow Ce^{3+} + H^+$. Additional
317 experiments that explore the following mechanisms of substitution $Zr^{4+} \rightarrow Ce^{3+}$ + Li+ and Si^{4+} +
318 $Zr^{4+} \rightarrow P^{5+} + Ce^{3+}$ (Trail et al. 2016) are worth investigating. Also, there are no experiments that
319 quantify the preservation potential of Ce valence in zircons as a function of temperature. Even if
320 this method is discovered to have limited value for Hadean zircons, it may be useful for younger

samples. Multiple isotope dilution-TIMS ages obtained from carefully micro-fractured zircon growth domains are providing new insights into continuously changing histories of silicate magmas (Matzel et al., 2006; Rivera et al., 2013). Combining such high precision age measurements with micron-scale Ce valence quantification (Trail et al., 2015) may enable a direct assessment of changes in magma oxidation state that occur over timescales of zircon growth.

Hadean subaerial crust

When did a subaerial surfaces emerge and what evidence of it remains in the geologic record? The discovery of mature sedimentary rocks such as quartzites or conglomerates supports the existence of subaerial exposure, including the Eoarchean Inukjuak rocks (David et al., 2009; Cates et al 2013; cf. Oneil et al., 2013), though Eoarchean or Hadean siliciclastic sedimentary rocks older than 3.9 Ga have not yet been discovered.

However, it is understood that weathering of subaerial rocks results in a residuum enriched in Al, not Na, Ca, and K, which are water soluble. If this material is buried and assimilated into a magma, it is expected to produce melts enriched in Al relative to Na^{+}, Ca^{2+}, K^{+}; i.e., $Al_2O_3/(CaO+Na_2O+K_2O) > 1$, or peraluminous rocks. Hadean zircon inclusion mineralogy studies point to the presence of muscovite and biotite derived from peraluminous parent rocks (Mojzsis et al., 2001; Hopkins et al., 2008; 2010; Bell et al., 2017). These observations support the idea of Hadean subaerial continental crust because ~1-2% of Hadean samples contain primary muscovite inclusions that are exposed on the surfaces of polished grains (Bell et al., 2015a). Complementary to inclusion studies, Trail et al. (2017) quantified zircon Al contents by LA-ICP-MS and ion microprobe from metaluminous and peraluminous rocks from 18 different granitoids. The expectation is that zircons that crystallized in peraluminous melts

may have higher Al concentrations – as a trace impurity – than zircons derived from metaluminous silicate melts with $Al_2O_3/(CaO+Na_2O+K_2O)$ <1. Zircons from peraluminous rocks yield an average concentration of ~10 ppm Al, which defines a different distribution – though with overlap – than crystals found in metaluminous rocks (average ≈ 1.3 ppm). Limited application of these observations to the Hadean Jack Hills detrital zircon record suggests a peraluminous origin for one pre-3.9 Ga zircon (n = 39), while about 8% (out of 236 zircons analyzed) of the Archean zircons exhibit elevated Al concentrations consistent with peraluminous melts. The small number of pre-3.9 Ga data should be taken in context; these measurements need to be extended beyond the 40 zircons evaluated in this pilot study.

Recent experimental results involving zircon synthesis in a piston cylinder from granitic melts, with different ASI values but same temperature, pressure, and water content reinforce observations made in natural samples (Wang and Trail, 2017). For the metaluminous melts (T = 1150 ^{o}C) zircon Al concentrations were as low as ~30 ppm, whereas for the most peraluminous melts, concentrations are on the order of ~200 ppm. The notably higher Al concentration in experimental zircons compared with natural zircons (1 to 10 ppm), is likely due to the higher crystallization temperature, e.g., >1100°C, compared to <800°C, for most natural zircons. While future work seeks to parameterize the solubility of Al in zircon as function of temperature and melt composition, an ulterior goal will involve the characterization Al solubilities in zircon with the activities of Al_2SiO_5, SiO_2, and H_2O buffered. Trail et al. (2011b) showed that Al may substitute into the zircon lattice through the following reaction $Al^{3+} + H^{+} \rightarrow Si^{4+}$ and so H_2O activity might also control Al uptake in zircon. Presently, there is no evidence that alkalies charge compensate for Al substitution in zircon. For instance, there is no correlation between Al and Li concentrations in zircon (Trail et al., 2017), which suggests that Li incorporation into

zircon (or other alkalies) are mostly controlled by the presence of rare earth elements (Trail et al., 2016).

Si and O isotopes in zircon

About 75% of the crust is either Si or O by weight, and therefore the identity of weathered material strongly depends on lithospheric cycling of these two elements. Oxygen isotope measurements in silicate rocks are well established, and recent advances in analytical techniques are now at the precision required to resolve variations in igneous Si isotope compositions (e.g. Georg et al., 2006; Zambardi and Poitrasson, 2011; Savage et al., 2011, 2012). These two isotopic systems have the potential to significantly advance our understanding of silicate weathering during the Hadean and Eoarchean and to constrain the identity Hadean weathered material.

Moreover, in the absence of a sedimentary/evolved component, Si isotopic composition varies linearly with Si content in igneous rocks, with the more differentiated samples yielding higher δ^{30}Si values (Savage et al., 2011). In cumulate igneous rocks Si isotope compositions can be used to broadly predict the rock's normative mineralogy (Savage et al., 2013). Altogether, this information illustrates that the Si isotope composition of whole rocks record information of their past history, including weathering and magmatic differentiation.

To explore Si isotopes at the mineral scale, mineral-mineral Si isotope fractionation factors are needed. The magnitude and sense of Si isotope fractionation between zircon and quartz have been experimentally investigated based on the 3 isotope exchange method, in which zircon and quartz progressively approached their equilibrium isotopic composition. Direct

390 synthesis experiments similar to the zircon-quartz oxygen isotope fractionation study of Trail et
391 al. (2009) have also been conducted. Preliminary data yield calculated fractionations that are
392 broadly consistent with those measured between zircon-quartz pairs in natural samples (Trail and
393 Savage 2015, 2017); that is, δ^{30}Si(quartz) - δ^{30}Si(zircon) ≈ 0.4‰. With this information,
394 simultaneous multicollection of O and Si isotopes using the CAMECA *ims*1290 ion microprobe
395 at UCLA will add a new dimension to the nature of silicate weathering of the early crust (Figure
396 3b). Specifically, the goal is to better define the composition of Hadean material involved in
397 crust-atmosphere-hydrosphere interactions, which may include feslic/mafic sediments, chemical
398 sediments, and altered basalt.
399

400 ## Implications

401 Hadean zircon chemistry has transformed our view of the earliest Earth, even with full
402 awareness that our understanding is likely biased by the restricted provenance of the material thus
403 far explored. No single example highlights this more than the Jack Hills zircons, as the vast
404 majority of Hadean zircons studied in detail come from a single outcrop (Harrison et al., 2017).
405 These samples continue to serve an integral role in the quest to decipher early Earth
406 environments, though a more accurate picture of Hadean/Eoarchean surface states and
407 environments requires investigations that extend beyond single outcrops. There are 13 sites for
408 which pre-4.0 Ga material has been identified (Harrison, et al., 2017), which will surely lead to
409 information about the Hadean Earth if interrogated to the same level of detail as the Jack Hills.
410 As recorders of crustal evolution, perhaps the most intriguing aspect of Hadean zircon
411 chemistry is that many of them appear to have formed in volatile rich magmas that captured and
412 archived a fraction of Earth's ancient surface chemistry through re-melting of sediments. The

413 combination of Si- and O-isotopes together may lead to new insights that define the weathered
414 product with greater detail (Abraham et al. 2011). Given the prospect of a Hadean biosphere
415 (Bell et al., 2015b), reconstructions of the near surface environment may be essential to
416 understand the transition from prebiotic to biotic chemistry.
417
418
419 For instance, the presence (and abundance) of subaerial continental exposure is important
420 for some origin of life models. First, subaerial weathering of continental crust may have provided
421 key components (e.g., clays?) needed for early pre-biotic chemistry (Ferris and Ertem, 1993); Al
422 concentrations and Si-/O-isotope ratios in zircon will help define the identity of this material.
423 Second, the presence of subaerial exposures help facilitate model prebiotic chemical reactions
424 conducted in the laboratory. Consider, for example, that RNA may be a potentially important
425 link between prebiotic chemistry and modern DNA biochemistry (Zaug and Cech, 1986).
426 However, ribose, which is a major component of the RNA molecule, is unstable is many aqueous
427 environments. One possible solution to this dilemma centers on a geological model in which
428 RNA developed in an aqueous environment enriched in borate. Borate acts as a complexing
429 agent that effectively stabilizes ribose against decomposition in aqueous solutions. Specifically,
430 ribose is stabilized in solution in the presence of borate-buffering evaporate minerals such as
431 colemanite, $CaB_3O_4(OH)_3(H_2O)$, ulexite, $NaCaB_5O_6(OH)_6(H_2O)_5$, and kernite,
432 $Na_2B_4O_6(OH)_2(H_2O)_3$, implying a desert-like subaerial environment (Ricardo et al., 2004;
433 Benner et al., 2011). If the simple organic precursors existed, the presence of borate could have
434 allowed the accumulation of ribose in prebiotic environments. In this regard, evidence for

435 subaerial exposure, whether in the form of inclusion mineralogy or trace elements in zircon (Al)
436 is needed to support the above model.

437 Another question is whether complex molecules such as amino acids formed on the early
438 Earth. One of the first breakthroughs is the now-famous Miller-Urey experiment in which an
439 "atmosphere" comprised of the reducing gases methane (CH_4), ammonia (NH_3), and hydrogen
440 (H_2) were subjected to simulated lightning (Miller, 1953). In the mix of experimental products
441 were many of the amino acids that are major components of cells. Later experiments showed
442 that the products also contained high energy intermediates like cyanide and acetylene (Stribling
443 and Miller, 1987). This was an important observation because cyanide and acetylene can
444 assemble in subsequent steps to form nucleotides, which are the building blocks of genetic
445 material. Knowledge of the early atmospheric composition would enable researchers to explore
446 reaction pathways that could lead to molecules of increasing complexity such as amino acids, but
447 without knowledge of the reactants, the products of such experiments are of limited value. As
448 discussed, experiments help constrain volatiles emanating from the Hadean Earth, which
449 probably dominated by neutral species. While a useful constraint, defining the relative
450 abundance of possible reactants as inputs for Miller-Urey type experiments would benefit from a
451 more precise oxygen fugacity sensor, coupled with zircon-melt partition coefficients for elements
452 that comprise volatile species (vs. oxygen fugacity). While H in zircon has certain complications
453 (section 3.1), Harrison et al. (2017) speculated about the possible incorporation of C into natural
454 zircon.

455 The picture of the early Earth will likely become clearer as new geochemical tools and
456 additional crustal remnants are discovered. Some of these problems may not be solvable in
457 realistic timeframes, or may give sufficiently ambiguous results with limited value.

458 Nevertheless, models of the earliest Earth environmental conditions based on geochemical data
459 from this Eon should be held in preference.
460

461 ## Acknowledgements

462 I thank Mark Harrison and another reviewer for reviews and Elizabeth Bell for an unofficial
463 review. Mike Ackerson, Elizabeth Bell, Patrick Boehnke, Jacob Buettner, Mark Harrison, Ming-
464 Chang Liu, Martha Miller, Steve Mojzsis, Paul Savage, Nick Tailby, Jay Thomas, Yanling
465 Wang, and Bruce Watson are thanked for discussions and assistance. This work was supported
466 by NSF grants EAR-1447404, EAR-1545637 and EAR-1650033**,** and Collaborative for Research
467 in Origins (CRiO) at the University of Colorado Boulder, which is funded by the John
468 Templeton Foundation-FfAME Origins program. The ion microprobe facility at UCLA is
469 partially supported by a grant from the Instrumentation and Facilities Program, Division of Earth
470 Sciences, NSF (EAR-1734856).

471 ## References

472 S.S. Abbott, T.M. Harrison, A.K. Schmitt and S.J. Mojzsis (2012) A search for terrestrial
473 evidence of the Late Heavy Bombardment in Ti-U-Th-Pb depth profiles of ancient
474 zircons. Proc. Nat. Acad. Sci. 109, 13,486-13,492
475 Abraham, K. et al., (2011) Coupled silicon–oxygen isotope fractionation traces Archaean
476 silicification. Earth and Planetary Science Letters, 301, 222-230.
477 Amelin, Y. 2004. Sm-Nd systematics of zircon. Chemical Geology, 211, 375-387.
478 Barboni, M. et al., (2017) Early formation of the Moon 4.51 billion years ago. Science Advances,
479 3, e1602365.

480 Bell, D.R., (2004) Abundance and Partitioning of OH in a High-pressure Magmatic System:
481 Megacrysts from the Monastery Kimberlite, South Africa. Journal of Petrology, 45(8),
482 1539-1564.
483 Bell, E.A., Boehnke, P., Hopkins-Wielicki, M.D., and Harrison, T.M. (2015a) Distinguishing
484 primary and secondary inclusion assemblages in Jack Hills zircons. Lithos, 234-235, 15-
485 26.
486 Bell, E.A., Boehnke, P., and Harrison, T.M., (2015b) Potentially biogenic carbon preserved in a
487 4.1 billion-year-old zircon. Proc Natl Acad Sci, 112: 14518–14521.
488 Bell, E.A., Boehnke, P., and Harrison, T.M., (2017) Applications of biotite inclusion
489 composition to zircon provenance determination. Earth and Planetary Science Letters,
490 473, 237-246.
491 Bell, E.A., Harrison, T.M., McCulloch, M.T., and Young, E.D. (2011) Early Archean crustal
492 evolution of the Jack Hills Zircon source terrane inferred from Lu–Hf, 207Pb/206Pb, and
493 δ18O systematics of Jack Hills zircons. Geochimica et Cosmochimica Acta, 75(17),
494 4816-4829.
495 Benner, S.A., Kim, H.-J., and Carrigan, M.A. (2012) Asphalt, Water, and the Prebiotic Synthesis
496 of Ribose, Ribonucleosides, and RNA. Accounts of Chemical research, 45, 2025–2034.
497 Burgisser, A., and Scaillet, B. (2007) Redox evolution of a degassing magma rising to the
498 surface. Nature, 445, 194-197.
499 Burnham, A.D., and Berry, A.J., (2012) An experimental study of trace element partitioning
500 between zircon and melt as a function of oxygen fugacity. Geochimica et Cosmochimica
501 Acta, 95, 196-212.

Canil, D., (1997) Vanadium partitioning and the oxidation state of Archaean komatiite magmas. Nature, 389, 842-845.

Carmichael, I.S., and Ghiorso, M., (1990) The effect of oxygen fugacity on the redox state of natural liquids and their crystallizing phases. Reviews in Mineralogy and Geochemistry, 24(1), 191-212.

Caro, G., Morino, P., Mojzsis, S.J., Cates, N.L., and Bleeker, W. (2017) Sluggish Hadean geodynamics: Evidence from coupled 146,147 Sm– 142,143 Nd systematics in Eoarchean supracrustal rocks of the Inukjuak domain (Québec). Earth and Planetary Science Letters, 457, 23-37.

Cates, N.L., and Mojzsis, S.J. (2009) Metamorphic zircon, trace elements and Neoarchean metamorphism in the ca. 3.75 Ga Nuvvuagittuq supracrustal belt, Québec (Canada). Chemical Geology, 261, 99-114.

Cates, N.L., Ziegler, K., Schmitt, A.K., and Mojzsis, S.J. (2013) Reduced, reused and recycled: Detrital zircons define a maximum age for the Eoarchean (ca. 3750–3780Ma) Nuvvuagittuq Supracrustal Belt, Québec (Canada). Earth and Planetary Science Letters, 362, 283-293.

Cavosie, A.J., Valley, J.W., and Wilde, S.A. (2006) Correlated microanalysis of zircon: Trace element, δ18O, and U–Th–Pb isotopic constraints on the igneous origin of complex >3900Ma detrital grains. Geochimica et Cosmochimica Acta, 70, 5601-5616.

Cavosie, A.J., Valley, J.W., Wilde, S.A., and E.I.M.F. (2005) Magmatic δ18O in 4400–3900 Ma detrital zircons: A record of the alteration and recycling of crust in the Early Archean. Earth and Planetary Science Letters, 235, 663-681.

524 Cavosie, A.J., Wilde, S.A., Liu, D., Weiblen, P.W., and Valley, J.W. (2004) Internal zoning and
525 U–Th–Pb chemistry of Jack Hills detrital zircons: a mineral record of early Archean to
526 Mesoproterozoic (4348–1576Ma) magmatism. Precambrian Research, 135, 251-279.
527 Cherniak, D.J., (2010) Diffusion in Accessory Minerals: Zircon, Titanite, Apatite, Monazite and
528 Xenotime. Reviews in Mineralogy and Geochemistry, 72, 827-869.
529 Connolly, J., and Cesare, B. (1993) C-O-H-S fluid composition and oxygen fugacity in graphitic
530 metapelites. Journal of Metamorphic Geology, 11, 379-388.
531 Darling, J.R., Moser, D.E., Heaman, L.M., Davis, W.J., O'Neil, J.O., Carlson, R. (2013)
532 Eoarchean to Neoarchean evolution of the Nuvvuagittuq supracrustal bet: New insights
533 from U-Pb zircon geochronology. 313 844-876.
534 David, J., Godin, L., Stevenson, R.K., O'Neil, J., and Francis, D. (2009) U-Pb ages (3.8–2.7 Ga)
535 and Nd isotope data from the newly identified Eoarchean Nuvvuagittuq supracrustal belt,
536 Superior Craton, Canada. Geological Society of America Bulletin, 121, 150-163.
537 de Hoog, J.C.M. et al. (2014) Hydrogen incorporation and charge balance in natural zircon.
538 Geochimica et Cosmochimica Acta, 141, 472-486.
539 Delano, J.W. (2001) Redox history of the Earth's interior since~ 3900 Ma: implications for
540 prebiotic molecules. Origins of Life and Evolution of the Biosphere, 31, 311-341.
541 Ferris, J.P., and Ertem, G., (1993) Montmorillonite catalysis of RNA oligomer formation in
542 aqueous solution. A model for the prebiotic formation of RNA. Journal of the American
543 Ceramic Society, 115: 12270–12275.
544 Ferriss, E.D.A., Essene, E.J., and Becker, U. (2008). Computational study of the effect of
545 pressure on the Ti-in-zircon geothermometer. European Journal of Mineralogy, 20, 745-
546 755.

547 Ferry, J.M., and Watson, E.B. (2007) New thermodynamic models and revised calibrations for
548 the Ti-in-zircon and Zr-in-rutile thermometers. Contributions to Mineralogy and
549 Petrology, 154, 429-437.
550 Frost, B.R. (1991) Introduction to oxygen fugacity and its petrologic importance. Reviews in
551 Mineralogy and Geochemistry, 25, 1-9.
552 Georg, R.B., Reynolds, B.C., Frank, M., and Halliday, A.N., (2006) New sample preparation
553 techniques for the determination of Si isotopic compositions using MC-ICPMS.
554 Chemical Geology, 235, 95-104.
555 Greer, J. (2013) Multiple generations of granitoid gneisses hosting supracrustal belts in the
556 Archean Inukjuak domain (Quebec, Canada). MS Thesis, University of Colorado,
557 Boulder.
558 Haggerty, S.E., Raber, E., Naeser, C.W., (1983) Fission track dating of kimberlitic zircons. Earth
559 and Planetary Science Letters, 63, 41-50.
560 Harrison, T.M. (2009) The Hadean Crust: Evidence from >4 Ga Zircons. Annual Review of
561 Earth and Planetary Sciences, 37, 479-505.
562 Harrison, T.M., Bell, E.A., and Boehnke, P. (2017) Hadean Zircon Petrochronology. Reviews in
563 Mineralogy and Geochemistry, 83, 329–363.
564 Harrison, T.M., Schmitt, A.K., McCulloch, M.T., and Lovera, O.M. (2008) Early (≥4.5 Ga)
565 formation of terrestrial crust: Lu–Hf, δ18O, and Ti thermometry results for Hadean
566 zircons. Earth and Planetary Science Letters, 268, 476-486.
567 Holden, P. et al. (2009) Mass-spectrometric mining of Hadean zircons by automated SHRIMP
568 multi-collector and single-collector U/Pb zircon age dating: The first 100,000 grains.
569 International Journal of Mass Spectrometry, 286, 53-63.

570 Hopkins, M., Harrison, T.M., and Manning, C.E., (2008) Low heat flow inferred from >4 Gyr
571 zircons suggests Hadean plate boundary interactions. Nature, 456, 493-496.
572 Hopkins, M.D., Harrison, T.M., Manning, C.E., (2010) Constraints on Hadean geodynamics
573 from mineral inclusions in >4Ga zircons. Earth and Planetary Science Letters, 298, 367-
574 376.
575 Ireland, T., and Wlotzka, F., (1992) The oldest zircons in the solar system. Earth and Planetary
576 Science Letters, 109, 1-10.
577 Kasting, J.F. (1993) Earth's early atmosphere. Science, 259, 920-926.
578 Kita, N.T., Ushikubo, T., Fu, B., and Valley, J.W. (2009) High precision SIMS oxygen isotope
579 analysis and the effect of sample topography. Chemical Geology, 264, 43-57.
580 Maas, R., Kinny, P.D., Williams, I.S., Froude, D.O., and Compston, W. (1992) The Earth's
581 oldest known crust: A geochronological and geochemical study of 3900-4200 Ma old
582 detrital zircons from Mt. Narryer and Jack Hills, Western Australia. Geochim.
583 Cosmochim. Acta, 56, 1281-1300.
584 Matzel, J.E.P., Bowring, S.A., and Miller, R.B. (2006) Time scales of pluton construction at
585 differing crustal levels: Examples from the Mount Stuart and Tenpeak intrusions, North
586 Cascades, Washington. Geological Society of America Bulletin, 118, 1412-1430.
587 Miller, S.L. (1953) A Production of Amino Acids under Possible Primitive Earth Conditions.
588 Science, 117, 528-529.
589 Mojzsis, S.J. et al., (2014) Component geochronology in the polyphase ca. 3920Ma Acasta
590 Gneiss. Geochimica et Cosmochimica Acta, 133, 68-96.
591 Mojzsis, S.J., Harrison, T.M., and Pidgeon, R.T. (2001) Oxygen-isotope evidence from ancient
592 zircons for liquid water at the Earth's surface 4,300 Myr ago. Nature, 409, 178-181.

593 O'Neil, J., Carlson, R.W., Francis, D., and Stevenson, R.K. (2008) Neodymium-142 evidence for
594 Hadean mafic crust. Science, 321, 1828-1831.
595 O'Neil, J., Boyet, M., Carlson, R.W., and Paquette, J.-L., (2013) Half a billion years of
596 reworking of Hadean mafic crust to produce the Nuvvuagittuq Eoarchean felsic crust.
597 Earth and Planetary Science Letters, 379, 13-25.
598 Paces, J.B., and Miller, J.D. (1993) Precise U-Pb ages of Duluth Complex and related mafic
599 intrusions, northeastern Minnesota: Geochronological insights to physical, petrogenetic,
600 paleomagnetic, and tectonomagmatic processes associated with the 1.1 Ga Midcontinent
601 Rift System. Journal of Geophysical Research: Solid Earth, 98(B8), 13997-14013.
602 Ricardo, A., Carrigan, M.A., Olcott, A.N., A., and Benner, S. (2004) Borate Minerals Stabilize
603 Ribose. Science, 303, 196.
604 Rivera, T.A., Storey, M., Schmitz, M.D., and Crowley, J.L. (2013) Age intercalibration of
605 40Ar/39Ar sanidine and chemically distinct U/Pb zircon populations from the Alder
606 Creek Rhyolite Quaternary geochronology standard. Chemical Geology, 345, 87-98.
607 Roth, A.S.G. et al. (2013) Inherited 142Nd anomalies in Eoarchean protoliths. Earth and
608 Planetary Science Letters, 361, 50-57.
609 Savage, P.S., Georg, R.B., Williams, H.M., Burton, K.W., and Halliday, A.N. (2011) Silicon
610 isotope fractionation during magmatic differentiation. Geochimica et Cosmochimica
611 Acta, 75, 6124-6139.
612 Savage, P.S., Georg, R.B., Williams, H.M., and Halliday, A.N. (2013) Silicon isotopes in
613 granulite xenoliths: insights into isotopic fractionation during igneous processes and the
614 composition of the deep continental crust. Earth and Planetary Science Letters, 365, 221-
615 231.

616 Savage, P.S. et al. (2012) The silicon isotope composition of granites. Geochimica et
617 Cosmochimica Acta, 92, 184-202.
618 Shannon, R.T. (1976) Revised effective ionic radii and systematic studies of interatomic
619 distances in halides and chalcogenides. Acta Crystallographica Section A: Crystal
620 Physics, Diffraction, Theoretical and General Crystallography, 32, 751-767.
621 Smythe, D.J., and Brenan, J.M., (2016) Magmatic oxygen fugacity estimated using zircon-melt
622 partitioning of cerium. Earth and Planetary Science Letters, 453, 260-266.
623 Stribling, R., and Miller, S.L., (1987) Energy yields for hydrogen cyanide and formaldehyde
624 syntheses: the HCN and amino acid concentrations in the primitive ocean. Origins of Life
625 and Evolution of the Biosphere, 17: 261-273.
626 Tailby, N.D. et al., (2011) Ti site occupancy in zircon. Geochimica et Cosmochimica Acta,
627 75(3), 905-921.
628 Thern, E.R., and Nelson, D.R. (2012) Detrital zircon age structure within ca. 3 Ga
629 metasedimentary rocks, Yilgarn Craton: Elucidation of Hadean source terranes by
630 principal component analysis. Precambrian Research, 214-215, 28-43.
631 Trail, D. et al. (2007) Constraints on Hadean zircon protoliths from oxygen isotopes, Ti-
632 thermometry, and rare earth elements. Geochemistry, Geophysics, Geosystems, 8,
633 Q06014, 1-22.
634 Trail, D., Bindeman, I.N., Watson, E.B., and Schmitt, A.K. (2009). Experimental calibration of
635 oxygen isotope fractionation between quartz and zircon. Geochimica et Cosmochimica
636 Acta, 73, 7110-7126.
637 Trail, D., Watson, E.B., and Tailby, N.D., (2011a). The oxidation state of Hadean magmas and
638 implications for early Earth's atmosphere. Nature, 480, 79-82.

639 Trail, D., Thomas, J.B., and Watson, E.B. (2011b) The incorporation of hydroxyl into zircon.
640 American Mineralogist, 96, 60-67.
641 Trail, D., Watson, E.B., and Tailby, N.D., (2012) Ce and Eu anomalies in zircon as proxies for
642 the oxidation state of magmas. Geochimica et Cosmochimica Acta, 97, 70-87.
643 Trail, D., Watson, E.B., and Tailby, N.D. (2013) Insights into the Hadean Earth from
644 experimental studies of zircon. Journal of the Geological Society of India, 81, 605-636.
645 Trail, D. et al., (2015) Redox evolution of silicic magmas: Insights from XANES measurements
646 of Ce valence in Bishop Tuff zircons. Chemical Geology, 402, 77-88.
647 Trail, D., and Savage, P.S. (2015) Si isotopes in zircon from experiments, granites, and mantle-
648 derived samples. Goldschmidt 2015 (abstract).
649 Trail, D. et al. (2016) Li zoning in zircon as a potential geospeedometer and peak temperature
650 indicator. Contributions to Mineralogy and Petrology, 171(3). 1007/s00410-016-1238-8
651 Trail, D., and Savage P.S. (2017) Si isotope fractionations in igneous silicates. Goldschmidt
652 2017. (abstract)
653 Trail, D., Tailby, N., Wang, Y., Harrison, T.M., and Boehnke, P. (2017) Aluminum in zircon as
654 evidence for peraluminous and metaluminous melts from the Hadean to present.
655 Geochemistry, Geophysics, Geosystems, 10.1002/2016GC006794.
656 Trail, D. (2018) Redox-controlled dissolution of monazite in fluids and implications for phase
657 stability in the lithosphere. American Mineralogist, 103, 453-461.
658 Valley, J.W., Kinny, P.D, Schulze, D.J., Spicuzza, M.J., (1998) Zircon megacrysts from
659 kimberlite: oxygen isotope variability among mantle melts. Contrib Mineral Petrol, 133,
660 1-11.

661 Wang, Y., and Trail, D. (2017) Experimental evidence for use of aluminum in zircon as a new
662 tracer to distinguish peraluminous and metaluminous melts. AGU 2017.
663 Watson, E.B., and Harrison, T.M. (2005) Zircon thermometer reveals minimum melting
664 conditions on earliest Earth. Science, 308, 841-844.
665 Watson, E.B., Wark, D.A., and Thomas, J.B. (2006) Crystallization thermometers for zircon and
666 rutile. Contributions to Mineralogy and Petrology 151, 413-433.
667 Weiss B.P., et al. (2015) Pervasive Remagnetization of Detrital Zircon Host Rocks in the Jack
668 Hills, Western Australia and Implications for Records of the Early Geodynamo. Earth
669 Planet Sci Lett, 430, 115-128.
670 Wilde, S.A., Valley, J.W., Peck, W.H., and Graham, C.M., (2001) Evidence from detrital zircons
671 for the existence of continental crust and oceans on the Earth 4.4 Gyr ago. Nature, 409,
672 175-178.
673 Woodhead, J.A., Rossman, G.R., and Silver, L.T. (1991) The metamictization of zircon:
674 Radiation dose-dependent structural characteristics. American Mineralogist, 76, 74–82.
675 Zambardi, T., and Poitrasson, F., (2011) Precise Determination of Silicon Isotopes in Silicate
676 Rock Reference Materials by MC-ICP-MS. Geostandards and Geoanalytical Research,
677 35, 89-99.
678 Zaug, J. Cech, T.R. (1986) The Intervening Sequence RNA of Tetrahymena is an Enzyme.
679 Science, 231, 470-475.
680
681
682 **Figure Captions**
683

Figure 1 Sketch map, identifying the major geological units (David et al. 2009; O'Neil et al. 2013; Greer, 2013) and locations of sampled loose sediment. I226 and I247 were collected from small streams and I300 collected from the shore of a small lake. The Boizard suite is comprised of a heterogenous gneissic tonalite with ultra/mafic enclaves; zircon U-Pb geochronology yield ages of 2722 to 2750 Ma, and associated pegmatite dikes yield U-Pb monazite ages of 2688 Ma (David et al., 2009). The Voizel suite consists of tonalitic gneisses. The Nuvvuagittuq Supracrustal Belt (NSB), is dominated by volcano-sedimentary sequences (David et al., 2009). The Ukaliq Supracrustal Belt (USB) is located a few km north and east of the NSB; a detailed field map of the boxed in region is presented by Caro et al. (2017).

Figure 2. U-Pb geochronology of zircons separated from unconsolidated sediment, with ~85% of the ages (i.e., >2.65 Ga) reflecting the local geology (Figure 1). I226 (n = 207) and I247 (n = 84) were collected from small streams passing through the NSB. I300 (n = 165) was collected near the Ukalik Supracrustal Belt and contains a single grain with an age of 3.74 Ga, implying this belt may contain a sequence with Eoarchean zircons.

Figure 3. (a) U-Pb LA-ICP-MS geochronology of Jack Hills zircons collected from the classic locality (e.g., Weiss et al., 2015). Of the 275 zircons, 34 are older than 4.0 Ga or about 12 %. **(b)** Secondary Electron and cathodoluminescence images of a 4.06 Ga grain, polished after U-Pb geochronology. The remaining outline of the LA-ICP-MS pit is visible, and to the left are ion microprobe spot analyses of Si and O isotopes. **(c)** U-Pb LA-ICP-MS geochronology of whole, unpolished grains reveal a decrease in identified grains older than 4.0 Ga, possibly due to the

intersection of younger overgrowths. **(d)** Stereoscope images of whole grains with U-Pb ages and the location of LA-ICP-MS pits identified.

Figure 4. log (A_i, per mm of zircon thickness) showing that absorption, which is proportional to concentration, is inversely related to temperature. All zircons were synthesized in the simple H_2O-SiO_2-ZrO_2 system. The total absorption, A_i, is calculated after the procedure discussed in Trail et al. (2011b). The A_i is plotted here, rather than concentration, because of the need to re-quantify the absorption coefficient for zircon (de Hoog et al., 2014).

Figure 5. Polarized spectra for doubly-polished crystals. Both zircons were treated in cold HF. When the electric vector is parallel to c (E//c) vs. E//a, the synthetic zircon spectra exhibit clear changes in absorption bands. Absorption spectra for a Jack Hills zircon contains broadly similar features and intensity independent of whether E//c vs. E//a, suggesting that most of the "water" is isotopic and therefore likely to be secondary. Similar features were observed for four other Jack Hills zircons.

Figure 6. The total absorption, A_i, plotted vs. distance from the rim showing a broadly monotonic decrease in concentration for the Kimberely Pool zircon, though the same correlation for the smaller Orapa Botswana zircon is absent. Samples were double polished and measurements were taken //a from rim to core.

Figure 7 (a) Example Ce L_3 edge XANES absorption spectra of synthetic zircons and standards. The bottom two spectra are end-member standards used to model valence of the unknowns. The

729 reduced→oxidized series represent spectra collected from synthetic zircons buffered at FMQ-
730 3.4, FMQ+0.7, and FMQ+6.8 respectively. Spectra show increased abundances of Ce^{4+}, as
731 judged by comparisons with standard spectra, with increasing oxygen fugacity. All spectra are
732 normalized to remove concentration effects for direct comparison of valence. **(b)** Backscattered
733 electron image of synthesized grains and **(c)** APS beamline reflected light image during data
734 collection. The scale bar applies to both images.
735
736
737
738
739
740
741
742
743
744
745 **Figure 1.**

This is a preprint, the final version is subject to change, of the American Mineralogist (MSA)
Cite as Authors (Year) Title. American Mineralogist, in press.
DOI: https://doi.org/10.2138/am-2018-6462

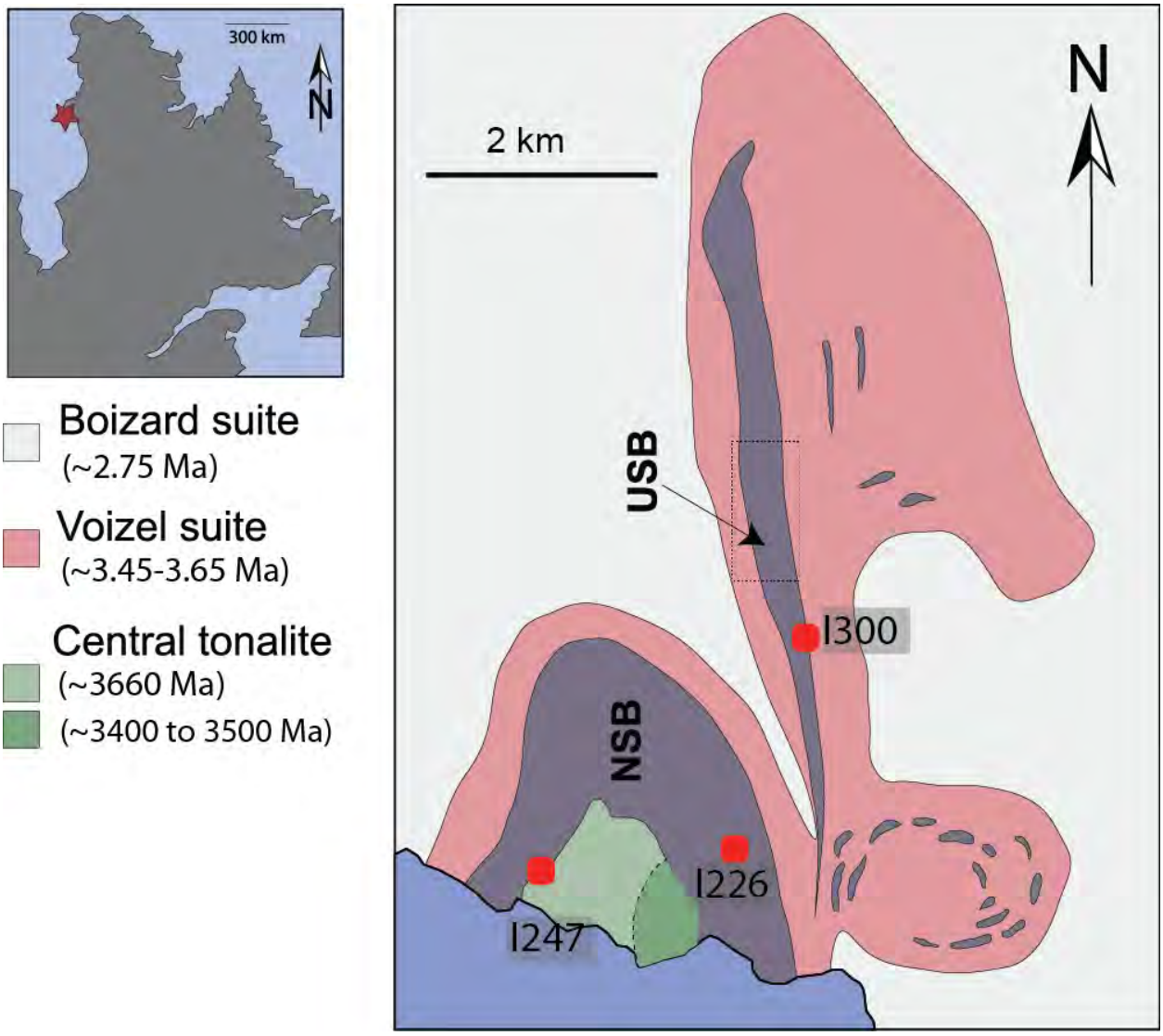

Figure 2

This is a preprint, the final version is subject to change, of the American Mineralogist (MSA)
Cite as Authors (Year) Title. American Mineralogist, in press.
DOI: https://doi.org/10.2138/am-2018-6462

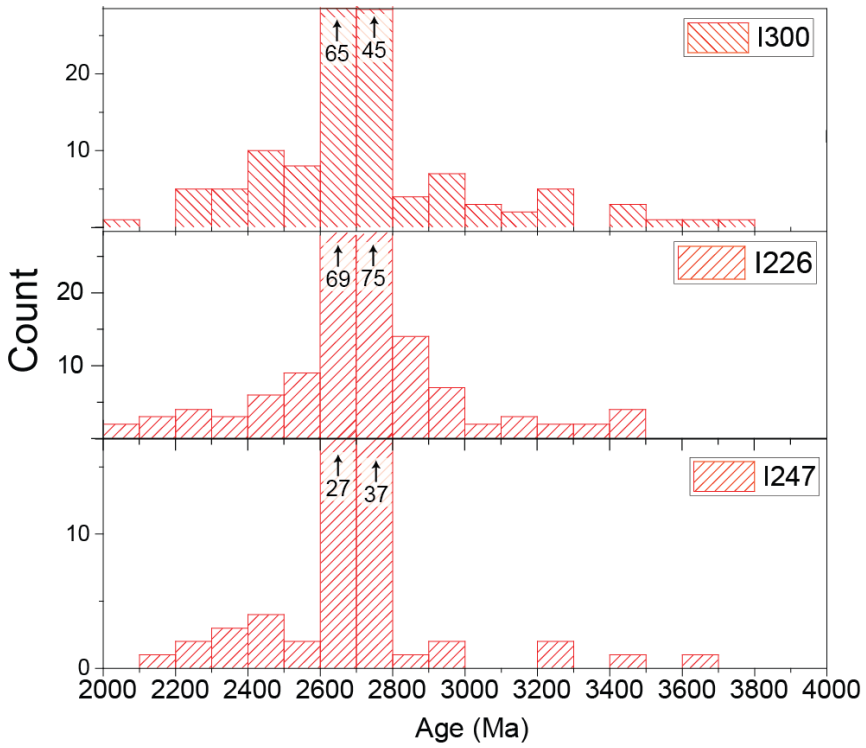

Figure 3.

This is a preprint, the final version is subject to change, of the American Mineralogist (MSA)
Cite as Authors (Year) Title. American Mineralogist, in press.
DOI: https://doi.org/10.2138/am-2018-6462

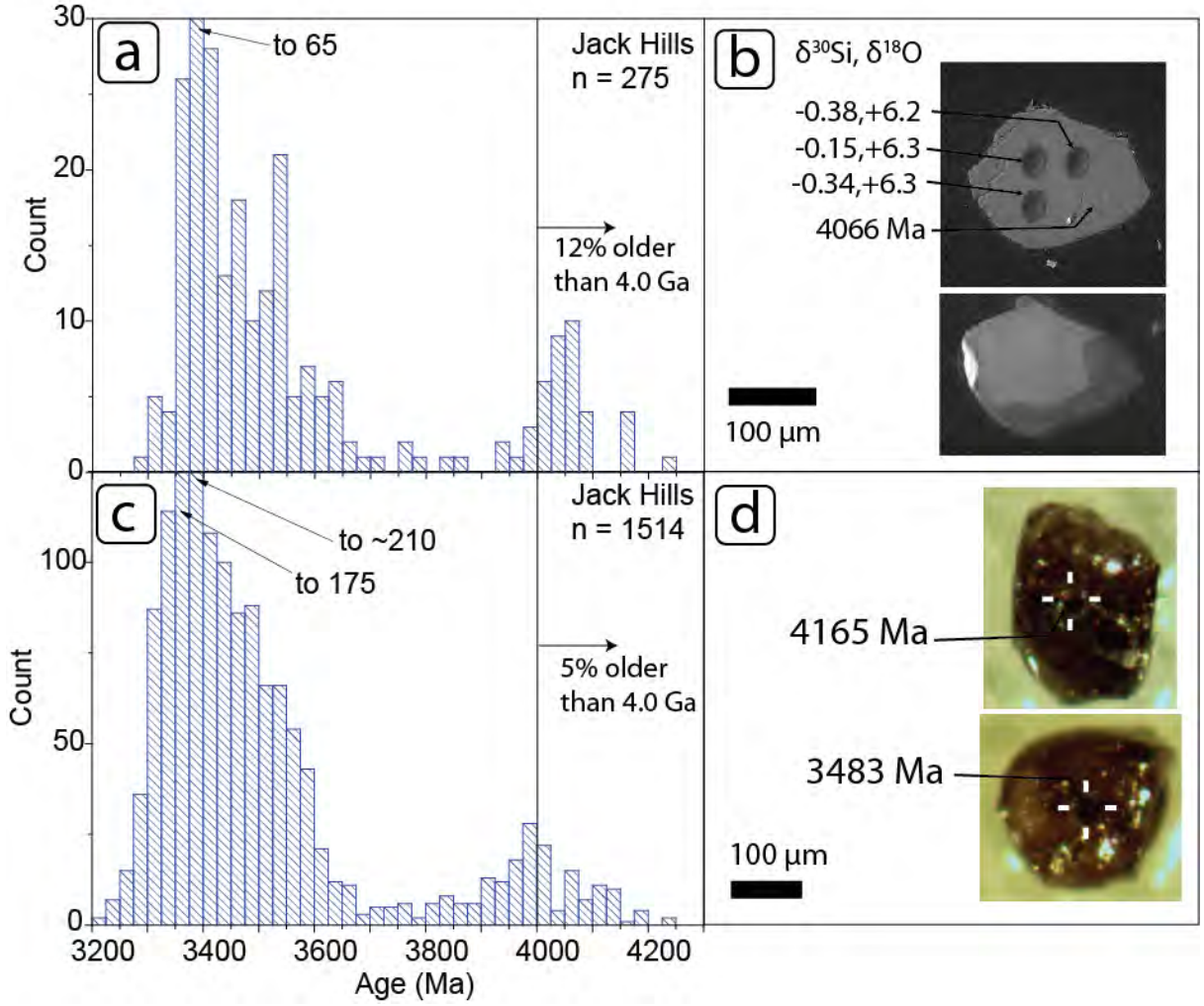

This is a preprint, the final version is subject to change, of the American Mineralogist (MSA)
Cite as Authors (Year) Title. American Mineralogist, in press.
DOI: https://doi.org/10.2138/am-2018-6462

779

780

781

782 **Figure 4**

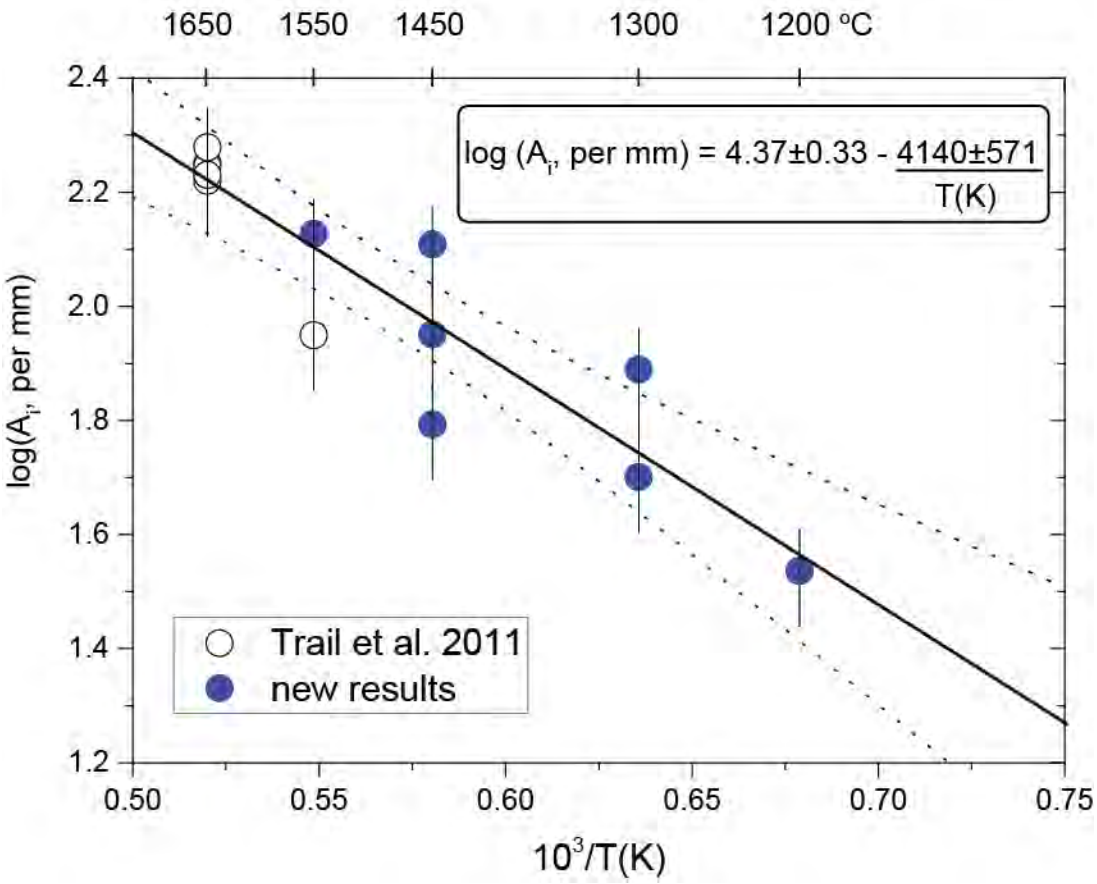

783

784

785

786

787

788

789

790

791

792

793

794 **Figure 5.**

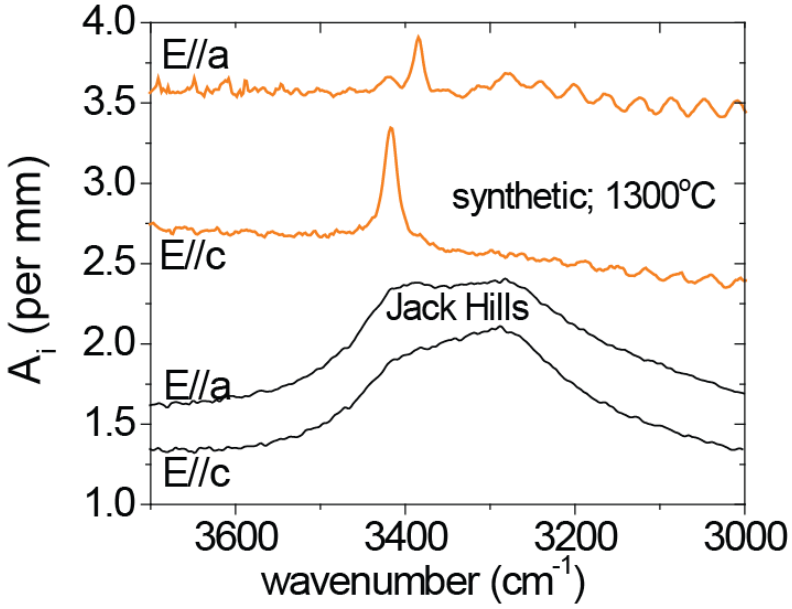

795

796

797

798

799

800

801

802

803

804

805

806

This is a preprint, the final version is subject to change, of the American Mineralogist (MSA)
Cite as Authors (Year) Title. American Mineralogist, in press.
DOI: https://doi.org/10.2138/am-2018-6462

807

808

809

810 **Figure 6**

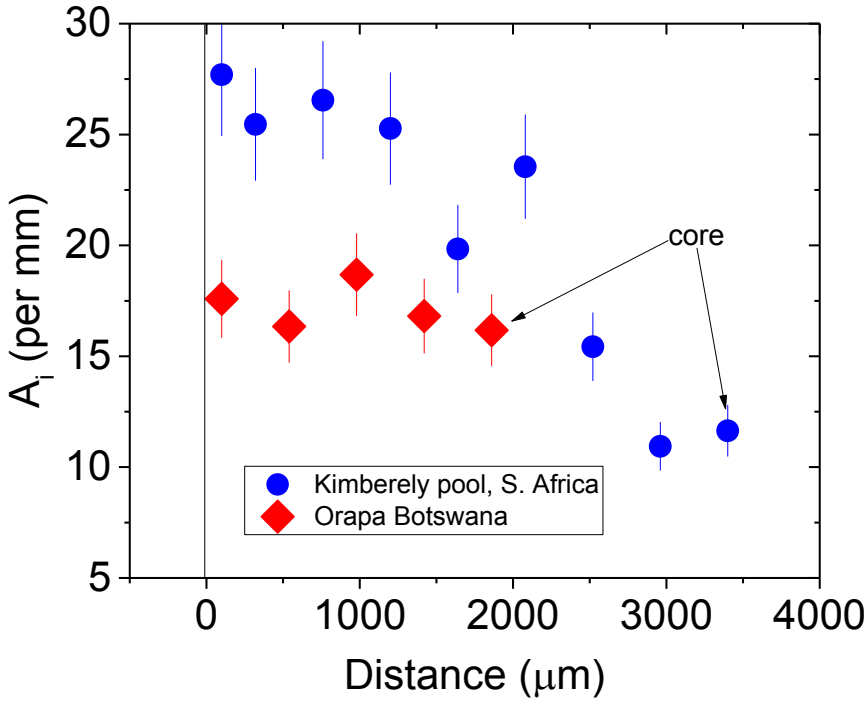

811

812

813

814

815

816

817

818

819

This is a preprint, the final version is subject to change, of the American Mineralogist (MSA)
Cite as Authors (Year) Title. American Mineralogist, in press.
DOI: https://doi.org/10.2138/am-2018-6462

820

821

822

823 **Figure 7**

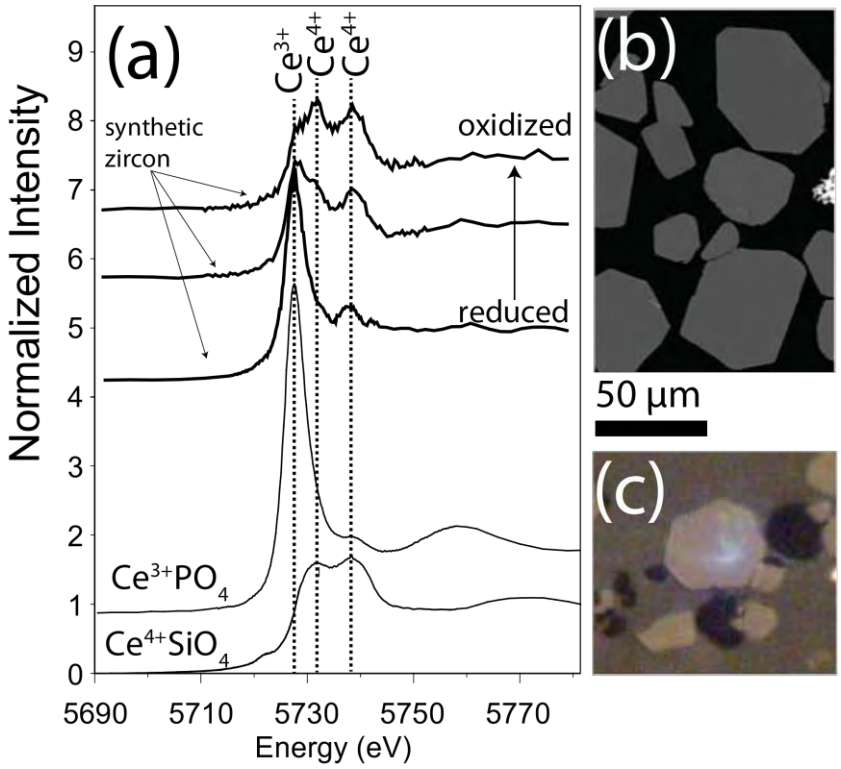

824

825